Neural Network Based Inverse Optimal Control for Uncertain Nonlinear System with Unmatched Disturbance

Jianan Liu, Zhongxin Fan, Shihua Li, and Rongjie Liu

***Abstract*—This paper addresses the problem of composite inverse optimal control for a class of uncertain nonlinear systems affected by unmatched disturbances. A control framework is proposed by integrating a generalized proportional integral observer (GPIO) with a neural network based scheme to simultaneously estimate both matched and mismatched disturbances and to approximate unknown system nonlinearities. To overcome the computational challenges associated with solving the nonlinear Hamilton-Jacobi-Bellman (HJB) equation in high-order systems, a composite adaptive inverse optimal control (IOC) strategy is developed. This approach combines GPIOs with the IOC framework, effectively utilizing the available system information while providing adaptive capability in dynamically changing environments. A rigorous theoretical analysis is presented to guarantee both stability and optimality of closed-loop system. The effectiveness and robustness of the proposed method are demonstrated through simulation studies.**

***Index Terms*—Inverse optimal control, neural network approximation, composite anti-disturbance control, generalized proportional integral observer**

I. Introduction

INVERSE optimal control provides a powerful theoretical framework for addressing inverse problems across the control systems, machine learning (ML), robotics, and optimization by leveraging optimality-based principles [1]. Since inverse optimal control [2] was introduced, it has undergone extensive research and development due to its ability to simultaneously ensure system stability and optimize control performance [3, 4]. However, practical engineering systems are frequently affected by unmodeled dynamics, unknown nonlinearities, and both matched and unmatched disturbances, making it challenging for conventional control approaches to achieve satisfactory performance [5]. Moreover, solving the Hamilton-Jacobi-Bellman (HJB) equation for high-dimensional nonlinear systems remains computationally prohibitive due to the "curse of dimensionality", which further complicates the controller design [6]. Therefore, designing robust and optimal control strategies without relying on precise system models remains a critical and unresolved challenge in current research.

The neural network (NN) based approximation is regarded as an effective method for handling unknown dynamics or system nonlinearities. To better understand how neural networks correspond to the structures of the compositional functions they aim to approximate, Ref. [7] introduced a synthetic algebraic framework along with a foundational theory of approximation. Directed acyclic graph (DAG) was employed to depict the input-output mapping, offering an intuitive visualization of compositional function structures. Motivated by the idea of Ref. [7], this paper adopts a DAG-based representation of the nonlinear system.

The presence of disturbances presents substantial challenges for optimal control in achieving desired closed-loop performance, including the minimization of steady-state errors and enhancement of dynamic response characteristics. In recent decades, various effective methods have been developed to mitigate disturbances in control systems.

Relevant works include disturbance observer design for nonlinear systems. Chen et al. [8] provided the first comprehensive and systematic overview and summary of existing disturbance/uncertainty estimation and attenuation techniques, with a particular focus on disturbance accommodation control (DAC) [9], disturbance observer based control (DOBC) [10–12], active disturbance rejection control (ADRC) [13–16], and composite hierarchical disturbance rejection control [17, 18]. Notably, the generalized proportional integral observer (GPIO) [19–21] has emerged as a particularly attractive solution, garnering significant research interest and widespread practical adoption owing to its unique capability of actively estimating and compensating for disturbances in real time. A composite sensorless control scheme was proposed for permanent magnet synchronous motors (PMSMs) based on generalized proportional integral observers and a Kalman filter, enabling high-precision back electromotive force estimation and robust position and speed estimation under disturbances [19]. A GPIO incorporated with a feedback domination approach was

Manuscript received: 20 January 2025; revised: 25 April 2025; accepted: 16 May 2025. *(Corresponding author: Shihua Li.)*

Citation: J. Liu, Z. Fan, S. Li, and R. Liu, Neural network based inverse optimal control for uncertain nonlinear system with unmatched disturbance, *Int. J. Intell. Control Syst.*, 2025, 30(2), 155–163.

Jianan Liu and Shihua Li are with School of Automation, Southeast University, Nanjing 210096, China, and also with Key Laboratory of Measurement and Control of Complex Systems of Engineering, Ministry of Education, Nanjing 210096, China (e-mail: ljn@seu.edu.cn; lsh@seu.edu.cn).

Zhongxin Fan is with SINOMACH Digital Technology Corporation, Nanjing 210023, China (e-mail: zhxfan@seu.edu.cn).

Rongjie Liu is with Department of Statistics, University of Georgia, Athens, GA 30602, USA (e-mail: rjliu@uga.edu).

Digital Object Identifier 10.62678/IJICS202506.10160

designed to compensate for disturbance and suppress nonlinear uncertainty for nonlinear uncertain systems with time-varying disturbances [20]. Yuan et al. [21] presented a GPIO-based sliding mode control approach for regulating the high-pressure common rail system in diesel engines.

This paper proposes a novel composite adaptive inverse optimal control framework that integrates a GPIO with a neural network based estimation scheme. The GPIO is employed to estimate both matched and unmatched disturbances in real time, while the neural network is utilized to approximate unknown nonlinear dynamics, thereby reducing dependence on accurate system models. Compared to existing works, the contributions of this paper can be summarized as follows:

(1) A unified control structure is designed to integrate disturbance observation with inverse optimal control, thereby achieving both robustness and performance optimization.

(2) System uncertainties are adaptively learned using neural networks, which eliminates the need for analytically solving the HJB equation.

(3) A composite controller is developed to simultaneously handle both matched and unmatched disturbances, thereby enhancing the disturbance rejection capability of the closed-loop system.

A rigorous proof is provided to demonstrate the asymptotic stability and inverse optimality of the proposed control system. Symbols and their meanings are given in Table 1. In contrast to traditional sliding mode control [22] and adaptive backstepping method [23], the proposed strategy offers a more favorable trade-off between computational complexity and control accuracy. Simulation results in Section IV demonstrate that the proposed method maintains superior performance under multiple disturbance sources and parameter uncertainties.

The paper is organized as follows. Section II introduces the problem formulation and necessary preliminaries. Section III presents the GPIO design and the neural network based composite control strategy. Section IV demonstrates the effectiveness of the proposed approach through numerical simulations. Finally, Section V concludes the paper with the main works.

II. Problem Formulation

In this work, the following nonlinear control system confronted by uncertainty/disturbance is considered.

$$\begin{aligned} &\dot{x}_i = x_{i+1} + f_i(\bar{x}_i) + d_i(t),\ i = 1,2,\ldots,n-1; \\ &\dot{x}_n = u + f_n(\bar{x}_n) + d_n(t), \\ &y = x_1 \end{aligned} \tag{1}$$

where $x = [x_1, x_2, \ldots, x_n]^{\mathrm{T}} \in \mathbb{R}^n$, $u \in \mathbb{R}$, and $y \in \mathbb{R}$ are the system state, the control input, and the output, respectively. Initial condition is $x(0) = x_0$. For $i = 1,2,\ldots,n-1$, $f_i(\bar{x}_i)$ is the unknown continuous function defined on a compact set Ω to represent nonlinearities of Eq. (1), $\bar{x}_i = (x_1, x_2, \ldots, x_i)$. d_i, $i = 1,2,\ldots,n-1$, denotes the mismatched disturbance and d_n is a matched disturbance.

Table 1 Notation and physical meaning.

Symbol	Meaning
$x = [x_1, x_2, \ldots, x_n]^{\mathrm{T}}$	State vector
u	Control input
$y = x_1$	System output
$f_i(\bar{x}_i)$	Unknown nonlinearity, $\bar{x}_i = [x_1, x_2, \ldots, x_i]^{\mathrm{T}}$
$d_i(t)$	Mismatched disturbance, $i = 1,2,\ldots,n-1$
$d_n(t)$	Matched disturbance
$\tilde{f}_i(x)$	NN approximation of f_i
θ_i^* and $\hat{\theta}_i$	Ideal and estimated NN weights
$\tilde{\theta}_i$	Estimation error, $\theta_i^* - \hat{\theta}_i$
δ_i^*	Approximation error of NN
$\phi_i(x)$	NN basis function vector
$z_{i,j}$	GPIO state for x_i and $d_i^{(j)}$
$\lambda_{i,j}$	GPIO gain parameter
ϵ_i	Tracking error at step i
α_i	Virtual control law
P_i and Q_i	Lyapunov-related matrices
Γ_{ij}	Adaptation gain
σ_{ij}	Leakage coefficient
γ_i^*, $\hat{\gamma}_i$, and $\tilde{\gamma}_i$	NN gain and its estimate/error
E_i	Observer error vector
A_i and B_i	Observer system matrices
β_i	Bound on GPIO input term

Assumption 1 The disturbance $d(t)$ in Eq. (1) is differentiable and its higher derivative $d^{(j)}(t)$, $j = 1,2,\ldots,m$ satisfies $\lim\limits_{t\to\infty} d^{(j)}(t) = 0$.

Remark 1 To illustrate the rationality of the hypothesis, we take PMSM system as an example. All the parameters of the PMSM system are bounded and typically vary smoothly in practical applications. Moreover, the loading and unloading processes of the PMSM system are not instantaneous but occur gradually over time, i.e., these considerations collectively support the validity of Assumption 1.

Lemma 1 The globally input-to-state stable (ISS) nonlinear system $\dot{x} = G(x, v)$ ensures that if the control signal $v(t)$ converges to zero (i.e., $\lim\limits_{t\to\infty} v(t) = 0$), then the system state $x(t)$ will also asymptotically approach the origin (i.e., $\lim\limits_{t\to\infty} x(t) = 0$).

Consider Eq. (1) depicted by a network that involves multiple compositional functions. See Fig. 1 for details. By definition in Ref. [24], $h_{0,i}$, $i = 1,2,\ldots,n$ is the input node, $h_{1,i}$, $i = 1,2,\ldots,n$ is the hidden node, and $h_{2,i}$, $i = 1,2,\ldots,n$ is the ouput node. The hidden nodes involve unknown function f_i, $i = 1,2,\ldots,n$, making it impossible to accurately represent the functional relationship utilizing DAG based on algebraic theory. Hence, neural network approximation method is introduced as

$$\tilde{f}_i(x) = \theta_i^{*\mathrm{T}} \phi_i(x) + \delta_i^* \tag{2}$$

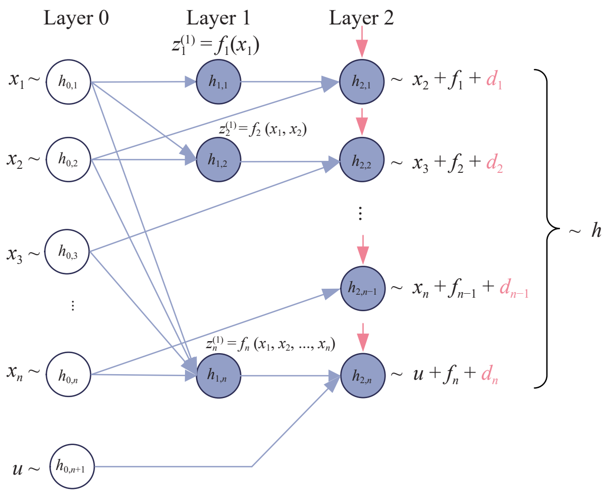

Figure 1 Function f_i, $i = 1,2,\ldots,n$ defined in Eq. (1).

with $|\phi_i| \leqslant \tau_i$ and $|\delta_i^*| \leqslant \bar{\delta}_i$. θ_i^* and δ_i^* represent the ideal weight vector and the approximation error, respectively. $\phi_i(x)$ is a vector-valued function composed of basic functions $\rho_i(x)$, $i = 1,2,\ldots,n$. Figure 2 gives a further description. Figure 3 illustrates the modified graph after substituting the nodes.

For a compositional function $(h, \mathcal{G}^h, \mathcal{L}^h)$ defined in Ref. [24], certain nodes requiring approximation can be replaced with shallow neural networks, resulting in the construction of a deep neural network. Proposition 1 presents an analysis of error propagation within the resulting directed acyclic graph structure.

Proposition 1 Let $L_2^h > 0$ denote the Lipschitz constant associated with the function h. Consider a collection of compositional functions $(\tilde{h}, \mathcal{G}^{\tilde{h}}, \mathcal{L}^{\tilde{h}})$, where $\tilde{h}$ shares the same domain as h and has a range suitable for composition. If the node h approximation error satisfies $|h(v) - \tilde{h}(v)| \leqslant \varepsilon$, then the overall approximation error is bounded by

$$\|h(x) - \tilde{h}(x)\|_p \leqslant L_2^h \varepsilon.$$

Here, $\tilde{h}$ is the resulting function after replacing h with its approximation $\tilde{h}$.

The proof refers to Ref. [24], which is omitted here.

III. Main Result

A. GPIO Design Process

Combining Eqs. (1) and (2), the generalized proportional integral observer is developed as

$$\begin{cases} \dot{z}_{i0} = z_{i1} + x_{i+1} + \hat{\theta}_i^{\mathrm{T}} \phi_i + \lambda_{i0}(x_i - z_{i0}), \\ \dot{z}_{i1} = z_{i2} + \lambda_{i1}(x_i - z_{i0}), \\ \vdots \\ \dot{z}_{im} = \lambda_{im}(x_i - z_{i0}) \end{cases} \tag{3}$$

where $i = 1,2,\ldots,n$, $x_{n+1} = u$, and $z_{i0}, z_{i1}, \ldots, z_{im}$ are the estimations of x_i, $d_i(t)$, $d_i^{(1)}(t)$, $\ldots$, $d_i^{(m)}(t)$, respectively. $\lambda_{i0}, \lambda_{i1}, \ldots, \lambda_{im} > 0$. Defining estimation errors $e_{i0} = x_i - z_{i0}$,

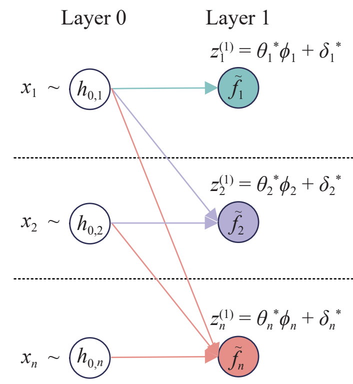

Figure 2 DAG corresponding to the neural network approximation function $\tilde{f}_i$, $i = 1,2,\ldots,n$.

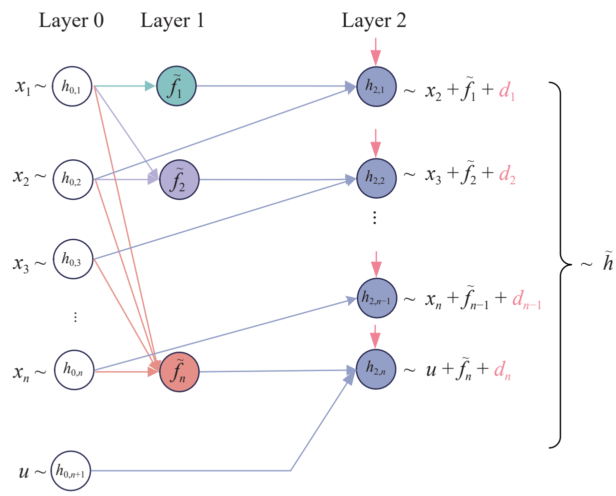

Figure 3 Compositional function formed by assigning the neural network approximation $\tilde{f}_i$, $i = 1,2,\ldots,n$ to nodes $h_{1,1}, h_{1,2}, \ldots, h_{1,n}$.

$e_{i1} = d_i - z_{i1}$, $\ldots$, $e_{im} = d_i^{(m-1)} - z_{im}$ and combining with Eq. (3), we get

$$\begin{cases} \dot{e}_{i0} = e_{i1} - \lambda_{i0} e_{i0}, \\ \dot{e}_{i1} = e_{i2} - \lambda_{i1} e_{i0}, \\ \vdots \\ \dot{e}_{im} = d_i^{(m)} - \lambda_{im} e_{i0} \end{cases} \tag{4}$$

We can rewrite Eq. (4) as

$$\dot{E}_i = A_i E_i + B_i \tag{5}$$

with

$$A_i = \begin{bmatrix} -\lambda_{i0} & 1 & 0 & \cdots & 0 \\ -\lambda_{i1} & 0 & 1 & \cdots & 0 \\ \vdots & \vdots & \vdots & \ddots & \vdots \\ -\lambda_{im} & 0 & 0 & \cdots & 1 \end{bmatrix}, \; B_i = \begin{bmatrix} 0 \\ \vdots \\ d_i^{(m)} \end{bmatrix}.$$

Here $E_i = [e_{i0}, e_{i1}, \ldots, e_{im}]^{\mathrm{T}} \in \mathbb{R}^{(m+1)\times 1}$ and $A_i \in \mathbb{R}^{(m+1)\times(m+1)}$ is a Hurwitz matrix. There exists a positive definite symmetric matrix $P_i \in \mathbb{R}^{(m+1)\times(m+1)}$ such that

$$A_i^{\mathrm{T}} P_i + P_i A_i = -Q_i \tag{6}$$

where $Q_i \in \mathbb{R}^{(m+1)\times(m+1)}$ is a positive definite matrix. With Eq. (6) and the fact that $E_i^{\mathrm{T}}E_i \geqslant \|E_i\|^2$ in mind, it is directly deduced that

$$2E_i^{\mathrm{T}}A_i^{\mathrm{T}}P_iE_i = E_i^{\mathrm{T}}(A_i^{\mathrm{T}}P_i + P_iA_i)E_i \leqslant -\lambda_{\min}(Q_i)\|E_i\|^2 \tag{7}$$

It is easy to find that B_i is bounded. Without loss of generality, assume $\|B_i\| \leqslant \beta_i$. $\beta_i > 0$ is a constant. Using the Cauchy-Schwarz inequality, one has

$$2E_i^{\mathrm{T}}P_1B_i \leqslant 2\beta_i\|P_i\|\|E_i\| \tag{8}$$

B. Adaptive Inverse Optimal Control Design

Step 1. Define $\epsilon_1 = x_1 - y_r$, $\tilde{\theta}_1 = \theta_1^* - \hat{\theta}_1$, $\tilde{\gamma}_1 = \gamma_1^* - \hat{\gamma}_1$, and choose the Lyapunov function as

$$V_1 = \frac{1}{2}\epsilon_1^2 + \frac{1}{2}\tilde{\theta}_1^{\mathrm{T}}\varGamma_{11}^{-1}\tilde{\theta}_1 + \frac{1}{2}\tilde{\gamma}_1^{\mathrm{T}}\varGamma_{12}^{-1}\tilde{\gamma}_1 + E_1^{\mathrm{T}}P_1E_1 \tag{9}$$

where $\varGamma_{11} > 0$, $\varGamma_{12} > 0$, and $P_1 > 0$. Then, the time derivative of V_1 along the trajectories of Eq. (1) is

$$\begin{aligned}\dot{V}_1 = {} & \epsilon_1(x_2 + \hat{\theta}_1^{\mathrm{T}}\phi_1 + z_{11} + \delta_1^* - \dot{y}_r) + \epsilon_1\tilde{\theta}_1^{\mathrm{T}}\phi_1 + \\ & \epsilon_1 e_{11} - \tilde{\theta}_1^{\mathrm{T}}\varGamma_{11}^{-1}\dot{\hat{\theta}}_1 - \tilde{\gamma}_1^{\mathrm{T}}\varGamma_{12}^{-1}\dot{\hat{\gamma}}_1 + \\ & 2E_1^{\mathrm{T}}A_1^{\mathrm{T}}P_1E_1 + 2E_1^{\mathrm{T}}P_1B_1\end{aligned} \tag{10}$$

Define $G_1 = -\dot{y}_r$, then G_1 can be approximated by $G_1 = W_1^{\mathrm{T}}\varPhi_1 + v_1 = T_1^{\mathrm{T}}\varTheta_1$, where $T_1 = [W_1, v_1]$ and $\varTheta_1 = [\varPhi_1\ 1]^{\mathrm{T}}$. We can deduce that

$$\begin{aligned}&\epsilon_1 G_1 \leqslant \frac{1}{2} + \epsilon_1\gamma_1^*\xi_1, \\ &\epsilon_1 e_{11} \leqslant \frac{1}{2}\epsilon_1^2 + \frac{1}{2}e_{11}^2, \\ &\epsilon_1\delta_1^* \leqslant \frac{1}{2}\epsilon_1^2 + \frac{1}{2}\bar{\delta}_1^2, \\ &\epsilon_1\hat{\theta}_1^{\mathrm{T}}\phi_1 \leqslant \frac{1}{2}\epsilon_1^2 + \tau_1^2\theta_1^{*2} + \tau_1^2\tilde{\theta}_1^2\end{aligned} \tag{11}$$

where $\gamma_1^* = W_1^2 + v_1^2$ and $\xi_1 = (\varTheta_1^{\mathrm{T}}\varTheta_1\epsilon_1)/2$. From Formulas (7), (8), and (11), one has

$$\begin{aligned}\dot{V}_1 \leqslant {} & \epsilon_1(\epsilon_2 + \alpha_1 + \hat{\gamma}_1\xi_1 + z_{11}) + \epsilon_1\tilde{\gamma}_1\xi_1 + \epsilon_1\tilde{\theta}_1^{\mathrm{T}}\phi_1 - \\ & \tilde{\theta}_1^{\mathrm{T}}\varGamma_{11}^{-1}\dot{\hat{\theta}}_1 - \tilde{\gamma}_1^{\mathrm{T}}\varGamma_{12}^{-1}\dot{\hat{\gamma}}_1 + \frac{3}{2}\epsilon_1^2 + \frac{1}{2}\bar{\delta}_1^2 + \frac{1}{2} + \\ & \tau_1^2\theta_1^{*2} + \tau_1^2\tilde{\theta}_1^2 - M_1\|E_1\|^2 + 2\beta_1\|P_1\|\|E_1\|\end{aligned} \tag{12}$$

where $\epsilon_2 = x_2 - \alpha_1$ and $M_1 = \lambda_{\min}(Q_1) - \dfrac{1}{2} > 0$. The virtual control law α_1 is designed as

$$\alpha_1 = -k_1\epsilon_1 - \frac{3}{2}\epsilon_1 - \frac{\varGamma_{12}^2\xi_1^2}{2}\epsilon_1 - \hat{\gamma}_1\xi_1 - z_{11} \tag{13}$$

where $k_1 > 0$. The updating laws are chosen as

$$\begin{aligned}&\dot{\hat{\theta}}_1 = \varGamma_{11}(\epsilon_1\phi_1 - \sigma_{11}\hat{\theta}_1), \\ &\dot{\hat{\gamma}}_1 = \varGamma_{12}(\epsilon_1\xi_1 - \sigma_{12}\hat{\gamma}_1)\end{aligned} \tag{14}$$

Note that

$$\begin{aligned}&\sigma_{11}\tilde{\theta}_1^{\mathrm{T}}\hat{\theta}_1 \leqslant \sigma_{11}\frac{\theta_1^{*2} - \tilde{\theta}_1^2}{2}, \\ &\sigma_{12}\tilde{\gamma}_1^{\mathrm{T}}\hat{\gamma}_1 \leqslant \sigma_{12}\frac{\gamma_1^{*2} - \tilde{\gamma}_1^2}{2}\end{aligned} \tag{15}$$

Substituting Formulas (13)–(15) into Formula (12) yields

$$\begin{aligned}\dot{V}_1 \leqslant {} & -k_1\epsilon_1^2 + \epsilon_1\epsilon_2 - \frac{\varGamma_{12}^2\xi_1^2}{2}\epsilon_1^2 + \sigma_{11}\tilde{\theta}_1^{\mathrm{T}}\hat{\theta}_1 + \sigma_{12}\tilde{\gamma}_1^{\mathrm{T}}\hat{\gamma}_1 + \\ & \frac{1}{2}\bar{\delta}_1^2 + \frac{1}{2} + \tau_1^2\theta_1^{*2} + \tau_1^2\tilde{\theta}_1^2 - \\ & M_1\|E_1\|^2 + 2\beta_1\|P_1\|\|E_1\| \leqslant \\ & -k_1\epsilon_1^2 - \frac{\varGamma_{12}^2\xi_1^2}{2}\epsilon_1^2 - \frac{\sigma_{11} - 2\tau_1^2}{2}\tilde{\theta}_1^2 - \frac{\sigma_{12}}{2}\tilde{\gamma}_1^2 + \\ & \frac{1}{2}\bar{\delta}_1^2 + \frac{1}{2} + \frac{\sigma_{11} + 2\tau_1^2}{2}\theta_1^{*2} + \frac{\sigma_{12}}{2}\gamma_1^{*2} + \epsilon_1\epsilon_2 - \\ & M_1\|E_1\|^2 + 2\beta_1\|P_1\|\|E_1\|\end{aligned} \tag{16}$$

Step 2. Choose the following Lyapunov function

$$V_2 = V_1 + \frac{1}{2}\epsilon_2^2 + \frac{1}{2}\tilde{\theta}_2^{\mathrm{T}}\varGamma_{21}^{-1}\tilde{\theta}_2 + \frac{1}{2}\tilde{\gamma}_2^{\mathrm{T}}\varGamma_{22}^{-1}\tilde{\gamma}_2 + E_2^{\mathrm{T}}P_2E_2 \tag{17}$$

where $\varGamma_{21} > 0$, $\varGamma_{22} > 0$, and $P_2 > 0$. Calculating the derivative of Eq. (17) yields

$$\begin{aligned}\dot{V}_2 \leqslant {} & -k_1\epsilon_1^2 - \frac{\varGamma_{12}^2\xi_1^2}{2}\epsilon_1^2 - \frac{\sigma_{11} - 2\tau_1^2}{2}\tilde{\theta}_1^2 - \frac{\sigma_{12}}{2}\tilde{\gamma}_1^2 + \\ & \epsilon_2\bigg(\epsilon_3 + \alpha_2 + \hat{\theta}_2^{\mathrm{T}}\phi_2 + z_{21} + \delta_2^* - \\ & \frac{\partial\alpha_1}{\partial\epsilon_1}\dot{\epsilon}_1 - \frac{\partial\alpha_1}{\partial z_{11}}\dot{z}_{11} - \frac{\partial\alpha_1}{\partial\hat{\gamma}_1}\dot{\hat{\gamma}}_1\bigg) + \\ & \epsilon_2\tilde{\theta}_2^{\mathrm{T}}\phi_2 + \epsilon_2 e_{21} - \tilde{\theta}_2^{\mathrm{T}}\varGamma_{21}^{-1}\dot{\hat{\theta}}_2 - \tilde{\gamma}_2^{\mathrm{T}}\varGamma_{22}^{-1}\dot{\hat{\gamma}}_2 + \\ & \frac{1}{2}\bar{\delta}_1^2 + \frac{1}{2} + \frac{\sigma_{11} + 2\tau_1^2}{2}\theta_1^{*2} + \frac{\sigma_{12}}{2}\gamma_1^{*2} + \epsilon_1\epsilon_2 - \\ & M_1\|E_1\|^2 + 2\beta_1\|P_1\|\|E_1\| + \\ & 2E_2^{\mathrm{T}}A_2^{\mathrm{T}}P_2E_2 + 2E_2^{\mathrm{T}}P_2B_2\end{aligned} \tag{18}$$

where $\epsilon_3 = x_3 - \alpha_2$. Define $G_2 = \epsilon_1 - \dfrac{\partial\alpha_1}{\partial\epsilon_1}\dot{\epsilon}_1 - \dfrac{\partial\alpha_1}{\partial z_{11}}\dot{z}_{11}$, then G_2 can be approximated by $G_2 = W_2^{\mathrm{T}}\varPhi_2 + v_2 = T_2^{\mathrm{T}}\varTheta_2$, where $T_2 = [W_2, v_2]$ and $\varTheta_2 = [\varPhi_2\ 1]^{\mathrm{T}}$. Let $\gamma_2^* = W_2^2 + v_2^2$ and $\xi_2 = \varTheta_2^{\mathrm{T}}\varTheta_2\epsilon_2/2$. Note that

$$\begin{aligned}&\epsilon_2 e_{21} \leqslant \frac{1}{2}\epsilon_2^2 + \frac{1}{2}e_{21}^2, \\ &\epsilon_2\delta_2^* \leqslant \frac{1}{2}\epsilon_2^2 + \frac{1}{2}\bar{\delta}_2^2, \\ &\epsilon_2 G_2 \leqslant \frac{1}{2} + \epsilon_2\gamma_2^*\xi_2, \\ &-\epsilon_2\frac{\partial\alpha_1}{\partial\hat{\gamma}_1}\dot{\hat{\gamma}}_1 \leqslant \epsilon_2^2\left(\frac{\partial\alpha_1}{\partial\hat{\gamma}_1}\right)^2 + \frac{\varGamma_{12}^2}{2}(\epsilon_1^2\xi_1^2 + 2\sigma_{12}^2\tilde{\gamma}_1^2 + \\ &\qquad 2\sigma_{12}^2\gamma_1^{*2}), \\ &\epsilon_2\hat{\theta}_2^{\mathrm{T}}\phi_2 \leqslant \frac{1}{2}\epsilon_2^2 + \tau_2^2\theta_2^{*2} + \tau_2^2\tilde{\theta}_2^2\end{aligned} \tag{19}$$

It can be deduced from Formulas (17)–(19) that

$$\begin{aligned}\dot{V}_2 \leqslant & -k_1\epsilon_1^2-\frac{\sigma_{11}-2\tau_1^2}{2}\tilde{\theta}_1^2-\frac{\sigma_{12}-2\Gamma_{12}^2\sigma_{12}^2}{2}\tilde{\gamma}_1^2+\\ & \epsilon_2(\epsilon_3+\alpha_2+\hat{\gamma}_2\xi_2+z_{21})+\epsilon_2\tilde{\gamma}_2\xi_2+\epsilon_2\tilde{\theta}_2^{\mathrm{T}}\phi_2-\\ & \tilde{\theta}_2^{\mathrm{T}}\Gamma_{21}^{-1}\dot{\hat{\theta}}_2-\tilde{\gamma}_2^{\mathrm{T}}\Gamma_{22}^{-1}\dot{\hat{\gamma}}_2+\frac{3}{2}\epsilon_2^2+\left(\frac{1}{2}\bar{\delta}_1^2+\frac{1}{2}\bar{\delta}_2^2\right)+\\ & \left(\frac{1}{2}+\frac{1}{2}\right)+\frac{\sigma_{11}+2\tau_1^2}{2}\theta_1^{*2}+\frac{\sigma_{12}+2\Gamma_{12}^2\sigma_{12}^2}{2}\gamma_1^{*2}+\\ & \epsilon_2^2\left(\frac{\partial\alpha_1}{\partial\hat{\gamma}_1}\right)^2+\tau_2^2\theta_2^{*2}+\tau_2^2\tilde{\theta}_2^2-\\ & (M_1\|E_1\|^2+M_2\|E_2\|^2)+\\ & 2(\beta_1\|P_1\|\|E_1\|+\beta_2\|P_2\|\|E_2\|)\end{aligned}\tag{20}$$

where $M_2=\lambda_{\min}(Q_2)-\dfrac{1}{2}>0$. Choose the virtual control law α_2 and updating law of $\hat{\theta}_2$ and $\hat{\gamma}_2$ as

$$\begin{aligned}&\alpha_2=-k_2\epsilon_2-\frac{3}{2}\epsilon_2-\frac{\Gamma_{22}^2\xi_2^2}{2}\epsilon_2-\frac{\partial\alpha_1}{\partial\hat{\gamma}_1}\epsilon_2-\hat{\gamma}_2\xi_2-z_{21},\\ &\dot{\hat{\theta}}_2=\Gamma_{21}(\epsilon_2\phi_2-\sigma_{21}\hat{\theta}_2),\\ &\dot{\hat{\gamma}}_2=\Gamma_{22}(\epsilon_2\xi_2-\sigma_{22}\hat{\gamma}_2)\end{aligned}\tag{21}$$

With the fact that

$$\begin{aligned}\sigma_{21}\tilde{\theta}_2^{\mathrm{T}}\hat{\theta}_2 &\leqslant \sigma_{21}\frac{\theta_2^{*2}-\tilde{\theta}_2^2}{2},\\ \sigma_{22}\tilde{\gamma}_2^{\mathrm{T}}\hat{\gamma}_2 &\leqslant \sigma_{22}\frac{\gamma_2^{*2}-\tilde{\gamma}_2^2}{2}\end{aligned}\tag{22}$$

there holds

$$\begin{aligned}\dot{V}_2 \leqslant & -(k_1\epsilon_1^2+k_2\epsilon_2^2)-\frac{\sigma_{11}-2\tau_1^2}{2}\tilde{\theta}_1^2-\frac{\sigma_{12}-2\Gamma_{12}^2\sigma_{12}^2}{2}\tilde{\gamma}_1^2+\\ & \epsilon_2\epsilon_3-\frac{\Gamma_{22}^2\xi_2^2}{2}\epsilon_2^2-\frac{\partial\alpha_1}{\partial\hat{\gamma}_1}\epsilon_2^2+\sigma_{21}\tilde{\theta}_2^{\mathrm{T}}\hat{\theta}_2+\sigma_{22}\tilde{\gamma}_2^{\mathrm{T}}\hat{\gamma}_2+\\ & \left(\frac{1}{2}\bar{\delta}_1^2+\frac{1}{2}\bar{\delta}_2^2\right)+\left(\frac{1}{2}+\frac{1}{2}\right)+\frac{\sigma_{11}+2\tau_1^2}{2}\theta_1^{*2}+\\ & \frac{\sigma_{12}+2\Gamma_{12}^2\sigma_{12}^2}{2}\gamma_1^{*2}+\epsilon_2^2\left(\frac{\partial\alpha_1}{\partial\hat{\gamma}_1}\right)^2+\tau_2^2\theta_2^{*2}+\tau_2^2\tilde{\theta}_2^2-\\ & (M_1\|E_1\|^2+M_2\|E_2\|^2)+\\ & 2(\beta_1\|P_1\|\|E_1\|+\beta_2\|P_2\|\|E_2\|)\leqslant\\ & -(k_1\epsilon_1^2+k_2\epsilon_2^2)-\left(\frac{\sigma_{11}-2\tau_1^2}{2}\tilde{\theta}_1^2+\frac{\sigma_{21}-2\tau_2^2}{2}\tilde{\theta}_2^2\right)-\\ & \frac{\sigma_{12}-2\Gamma_{12}^2\sigma_{12}^2}{2}\tilde{\gamma}_1^2-\frac{\sigma_{22}}{2}\tilde{\gamma}_2^2+\frac{1}{2}(\bar{\delta}_1^2+\bar{\delta}_2^2)+\\ & \left(\frac{1}{2}+\frac{1}{2}\right)+\left(\frac{\sigma_{11}+2\tau_1^2}{2}\theta_1^{*2}+\frac{\sigma_{21}+2\tau_2^2}{2}\theta_2^{*2}\right)+\\ & \frac{\sigma_{12}+2\Gamma_{12}^2\sigma_{12}^2}{2}\gamma_1^{*2}+\frac{\sigma_{22}}{2}\gamma_2^{*2}+\epsilon_2\epsilon_3-\\ & \frac{\Gamma_{22}^2\xi_2^2}{2}\epsilon_2^2-(M_1\|E_1\|^2+M_2\|E_2\|^2)+\\ & 2(\beta_1\|P_1\|\|E_1\|+\beta_2\|P_2\|\|E_2\|)\end{aligned}\tag{23}$$

Step i ($3\leqslant i\leqslant n$). Assume that the updating law and the virtual control law are well designed. The derivative of the Lyapunov function

$$V_i=V_{i-1}+\frac{1}{2}\epsilon_i^2+\frac{1}{2}\tilde{\theta}_i^{\mathrm{T}}\Gamma_{i1}^{-1}\tilde{\theta}_i+\frac{1}{2}\tilde{\gamma}_i^{\mathrm{T}}\Gamma_{i2}^{-1}\tilde{\gamma}_i+E_i^{\mathrm{T}}P_iE_i\tag{24}$$

satisfies

$$\begin{aligned}\dot{V}_i\leqslant & -\sum_{j=1}^{i}k_j\epsilon_j^2-\sum_{j=1}^{i}\frac{\sigma_{j1}-2\tau_j^2}{2}\tilde{\theta}_j^2-\\ & \sum_{j=1}^{i-1}\frac{\sigma_{j2}-2\Gamma_{j2}^2\sigma_{j2}^2}{2}\tilde{\gamma}_j^2-\frac{\sigma_{i2}}{2}\tilde{\gamma}_i^2+\\ & \frac{1}{2}\sum_{j=1}^{i}\bar{\delta}_j^2+\frac{i}{2}+\sum_{j=1}^{i}\frac{\sigma_{j1}+2\tau_j^2}{2}\theta_j^{*2}+\\ & \sum_{j=1}^{i-1}\frac{\sigma_{j2}+2\Gamma_{j2}^2\sigma_{j2}^2}{2}\gamma_j^{*2}+\frac{\sigma_{i2}}{2}\gamma_i^{*2}+\\ & \epsilon_i\epsilon_{i+1}-\frac{\Gamma_{i2}^2\xi_i^2}{2}\epsilon_i^2-\\ & \sum_{j=1}^{i}M_j\|E_j\|^2+2\sum_{j=1}^{i}\beta_j\|P_j\|\|E_j\|\end{aligned}\tag{25}$$

Obviously, Formula (25) reduces to Formula (23) when $i=2$. We claim that Formula (25) also holds at step $i+1$. Define $\epsilon_{i+2}=x_{i+2}-\alpha_{i+1}$ and the Lyapunov function

$$\begin{aligned}V_{i+1}=&V_i+\frac{1}{2}\epsilon_{i+1}^2+\frac{1}{2}\tilde{\theta}_{i+1}^{\mathrm{T}}\Gamma_{i+1,1}^{-1}\tilde{\theta}_{i+1}+\\ &\frac{1}{2}\tilde{\gamma}_{i+1}^{\mathrm{T}}\Gamma_{i+1,2}^{-1}\tilde{\gamma}_{i+1}+E_{i+1}^{\mathrm{T}}P_{i+1}E_{i+1}\end{aligned}\tag{26}$$

Then, it follows from Formula (25) that

$$\begin{aligned}\dot{V}_{i+1}\leqslant & -\sum_{j=1}^{i}k_j\epsilon_j^2-\sum_{j=1}^{i}\frac{\sigma_{j1}-2\tau_j^2}{2}\tilde{\theta}_j^2-\\ & \sum_{j=1}^{i-1}\frac{\sigma_{j2}-2\Gamma_{j2}^2\sigma_{j2}^2}{2}\tilde{\gamma}_j^2-\frac{\sigma_{i2}}{2}\tilde{\gamma}_i^2+\\ & \epsilon_{i+1}\Bigg(\epsilon_{i+2}+\alpha_{i+1}+\hat{\theta}_{i+1}^{\mathrm{T}}\phi_{i+1}+z_{i+1,1}+\\ & \delta_{i+1}^{*}-\frac{\partial\alpha_i}{\partial\epsilon_i}\dot{\epsilon}_i-\frac{\partial\alpha_i}{\partial z_{i1}}\dot{z}_{i1}-\frac{\partial\alpha_i}{\partial\hat{\gamma}_i}\dot{\hat{\gamma}}_i\Bigg)+\\ & \epsilon_{i+1}\tilde{\theta}_{i+1}^{\mathrm{T}}\phi_{i+1}+\epsilon_{i+1}e_{i+1,1}-\\ & \tilde{\theta}_{i+1}^{\mathrm{T}}\Gamma_{i+1,1}^{-1}\dot{\hat{\theta}}_{i+1}-\tilde{\gamma}_{i+1}^{\mathrm{T}}\Gamma_{i+1,2}^{-1}\dot{\hat{\gamma}}_{i+1}+\\ & \frac{1}{2}\sum_{j=1}^{i}\bar{\delta}_j^2+\frac{i}{2}+\sum_{j=1}^{i}\frac{\sigma_{j1}+2\tau_j^2}{2}\theta_j^{*2}+\\ & \sum_{j=1}^{i-1}\frac{\sigma_{j2}+2\Gamma_{j2}^2\sigma_{j2}^2}{2}\gamma_j^{*2}+\frac{\sigma_{i2}}{2}\gamma_i^{*2}+\\ & \epsilon_i\epsilon_{i+1}-\frac{\Gamma_{i2}^2\xi_i^2}{2}\epsilon_i^2-\\ & \sum_{j=1}^{i}M_j\|E_j\|^2+2\sum_{j=1}^{i}\beta_j\|P_j\|\|E_j\|\end{aligned}\tag{27}$$

Define $G_{i+1}=\epsilon_i-\dfrac{\partial\alpha_i}{\partial\epsilon_i}\dot{\epsilon}_i-\dfrac{\partial\alpha_i}{\partial z_{i1}}\dot{z}_{i1}$, then G_{i+1} can be approximated by $G_{i+1}=W_{i+1}^{\mathrm{T}}\Phi_{i+1}+v_{i+1}=T_{i+1}^{\mathrm{T}}\Theta_{i+1}$, where

$T_{i+1}=[W_{i+1},v_{i+1}]$ and $\Theta_{i+1}=[\Phi_{i+1}\ 1]^{\mathrm{T}}$. Let $\gamma^*_{i+1}=W^2_{i+1}+v^2_{i+1}$ and $\xi_{i+1}=\Theta^{\mathrm{T}}_{i+1}\Theta_{i+1}\epsilon_{i+1}/2$. The following inequalities can be deduced by utilizing the same manipulations in Formula (19)

$$\begin{aligned}
&\epsilon_{i+1}e_{i+1,1}\leqslant\frac{1}{2}\epsilon^2_{i+1}+\frac{1}{2}e^2_{i+1,1},\\
&\epsilon_{i+1}\delta^*_{i+1}\leqslant\frac{1}{2}\epsilon^2_{i+1}+\frac{1}{2}\bar{\delta}^2_{i+1},\\
&\epsilon_{i+1}G_{i+1}\leqslant\frac{1}{2}+\epsilon_{i+1}\gamma^*_{i+1}\xi_{i+1},\\
&-\epsilon_{i+1}\frac{\partial\alpha_i}{\partial\hat{\gamma}_i}\dot{\hat{\gamma}}_i\leqslant\epsilon^2_{i+1}\left(\frac{\partial\alpha_i}{\partial\hat{\gamma}_i}\right)^2+\frac{\Gamma^2_{i2}}{2}(\epsilon^2_i\xi^2_i+2\sigma^2_{i2}\tilde{\gamma}^2_i+\\
&\quad 2\sigma^2_{i2}\gamma^{*2}_i),\\
&\epsilon_{i+1}\hat{\theta}^{\mathrm{T}}_{i+1}\phi_{i+1}\leqslant\frac{1}{2}\epsilon^2_{i+1}+\tau^2_{i+1}{\theta^*_{i+1}}^2+\tau^2_{i+1}\tilde{\theta}^2_{i+1}
\end{aligned}\tag{28}$$

Substitute Formula (28) into Formula (27), and choose the virtual control law α_{i+1} and updating law of $\hat{\theta}_{i+1}$ and $\hat{\gamma}_{i+1}$ as

$$\begin{aligned}
\alpha_{i+1}=&-k_{i+1}\epsilon_{i+1}-\frac{3}{2}\epsilon_{i+1}-\frac{\Gamma^2_{i+1,2}\xi^2_{i+1}}{2}\epsilon_{i+1}-\\
&\left(\frac{\partial\alpha_i}{\partial\hat{\gamma}_i}\right)^2\epsilon_{i+1}-\hat{\gamma}_{i+1}\xi_{i+1}-z_{i+1,1},
\end{aligned}\tag{29}$$

$$\begin{aligned}
\dot{\hat{\theta}}_{i+1}&=\Gamma_{i+1,1}(\epsilon_{i+1}\phi_{i+1}-\sigma_{i+1,1}\hat{\theta}_{i+1}),\\
\dot{\hat{\gamma}}_{i+1}&=\Gamma_{i+1,2}(\epsilon_{i+1}\xi_{i+1}-\sigma_{i+1,2}\hat{\gamma}_{i+1})
\end{aligned}$$

With the fact that

$$\begin{aligned}
\sigma_{i+1,1}\tilde{\theta}^{\mathrm{T}}_{i+1}\hat{\theta}_{i+1}&\leqslant\sigma_{i+1,1}\frac{{\theta^*_{i+1}}^2-\tilde{\theta}^2_{i+1}}{2},\\
\sigma_{i+1,2}\tilde{\gamma}^{\mathrm{T}}_{i+1}\hat{\gamma}_{i+1}&\leqslant\sigma_{i+1,2}\frac{{\gamma^*_{i+1}}^2-\tilde{\gamma}^2_{i+1}}{2}
\end{aligned}\tag{30}$$

it is easy to verify that the following inequality holds.

$$\begin{aligned}
\dot{V}_{i+1}\leqslant&-\sum_{j=1}^{i+1}k_j\epsilon^2_j-\sum_{j=1}^{i+1}\frac{\sigma_{j1}-2\tau^2_j}{2}\tilde{\theta}^2_j-\\
&\sum_{j=1}^{i}\frac{\sigma_{j2}-2\Gamma^2_{j2}\sigma^2_{j2}}{2}\tilde{\gamma}^2_j-\frac{\sigma_{i+1,2}}{2}\tilde{\gamma}^2_{i+1}+\\
&\frac{1}{2}\sum_{j=1}^{i+1}\bar{\delta}^2_j+\frac{i+1}{2}+\sum_{j=1}^{i+1}\frac{\sigma_{j1}+2\tau^2_j}{2}\theta^{*2}_j+\\
&\sum_{j=1}^{i}\frac{\sigma_{j2}+2\Gamma^2_{j2}\sigma^2_{j2}}{2}\gamma^{*2}_j+\frac{\sigma_{i+1,2}}{2}{\gamma^*_{i+1}}^2+\\
&\epsilon_{i+1}\epsilon_{i+2}-\sum_{j=1}^{i+1}M_j\|E_j\|^2+2\sum_{j=1}^{i+1}\beta_j\|P_j\|\|E_j\|
\end{aligned}\tag{31}$$

In particular, at step n, we can obtain the actual control input

$$u=-k_n\epsilon_n-\epsilon_n-\left(\frac{\partial\alpha_{n-1}}{\partial\hat{\gamma}_{n-1}}\right)^2\epsilon_n-\hat{\gamma}_n\xi_n-z_{n1}\tag{32}$$

and the updating law is

$$\begin{aligned}
\dot{\hat{\theta}}_n&=\Gamma_{n1}(\epsilon_n\phi_n-\sigma_{n1}\hat{\theta}_n),\\
\dot{\hat{\gamma}}_n&=\Gamma_{n2}(\epsilon_n\xi_n-\sigma_{n2}\hat{\gamma}_n)
\end{aligned}\tag{33}$$

These render the Lyapunov function

$$V_n=V_{n-1}+\frac{1}{2}\epsilon^2_n+\frac{1}{2}\tilde{\theta}^{\mathrm{T}}_n\Gamma^{-1}_{n1}\tilde{\theta}_n+\frac{1}{2}\tilde{\gamma}^{\mathrm{T}}_n\Gamma^{-1}_{n2}\tilde{\gamma}_n+E^{\mathrm{T}}_nP_nE_n,$$

to satisfy

$$\begin{aligned}
\dot{V}_n\leqslant&-\sum_{j=1}^{n}k_j\epsilon^2_j-\sum_{j=1}^{n}\frac{\sigma_{j1}-2\tau^2_j}{2}\tilde{\theta}^2_j-\\
&\sum_{j=1}^{n-1}\frac{\sigma_{j2}-2\Gamma^2_{j2}\sigma^2_{j2}}{2}\tilde{\gamma}^2_j-\frac{\sigma_{n2}}{2}\tilde{\gamma}^2_n+\\
&\frac{1}{2}\sum_{j=1}^{n}\bar{\delta}^2_j+\frac{n}{2}+\sum_{j=1}^{n}\frac{\sigma_{j1}+2\tau^2_j}{2}\theta^{*2}_j+\\
&\sum_{j=1}^{n-1}\frac{\sigma_{j2}+2\Gamma^2_{j2}\sigma^2_{j2}}{2}\gamma^{*2}_j+\frac{\sigma_{n2}}{2}\gamma^{*2}_n-\\
&\sum_{j=1}^{n}M_j\|E_j\|^2+2\sum_{j=1}^{n}\beta_j\|P_j\|\|E_j\|
\end{aligned}\tag{34}$$

To illustrate the bounded property of the system state, Theorem 1 is developed.

Theorem 1 Considering Eq. (1), under the controller in Eq. (32), adaptive laws in Eqs. (14), (21), (29), and (33), and disturbance observer in Eq. (3), all signals of the closed-loop system are ultimately uniformly bounded.

Proof Choose the Lyapunov function as $V=V_n$ and the derivative of V is

$$\dot{V}\leqslant-aV+b\tag{35}$$

where

$$a=\min\{2k_j,\sigma_{j1}-2\tau^2_j,\sigma_{j2}-2\Gamma^2_{j2}\sigma^2_{j2},2M_j\|E_j\|^2,\sigma_{n2},j=1,2,\ldots,n\},$$

$$\begin{aligned}
b=&\frac{1}{2}\sum_{j=1}^{n}\bar{\delta}^2_j+\frac{n}{2}+\sum_{j=1}^{n}\frac{\sigma_{j1}+2\tau^2_j}{2}\theta^{*2}_j+\\
&\sum_{j=1}^{n-1}\frac{\sigma_{j2}+2\Gamma^2_{j2}\sigma^2_{j2}}{2}\gamma^{*2}_j+\frac{\sigma_{n2}}{2}\gamma^{*2}_n+2\sum_{j=1}^{n}\beta_j\|P_j\|\|E_j\|.
\end{aligned}$$

In addition, the bound can be obtained as $\lim\limits_{t\to\infty}\|\epsilon\|\leqslant(2b/a)^{\frac{1}{2}}$. This completes the whole proof. ■

C. Optimality Analysis

Based on the results acquired previously regarding the disturbance observer, updating law, and controller, we present an optimality analysis of the closed-loop system.

Theorem 2 Consider the composite stabilizing controller

$$u=u_c-z_{n1}\tag{36}$$

where u_c is a normal control input and z_{n1} is an estimated disturbance of d_n. For any $\beta\geqslant 2$, the modified control law

$$u^*_c=\beta u_c\tag{37}$$

solves the inverse optimal control problem.

Proof To show inverse optimality, we connect the closed-loop dynamics with an HJB-related framework. According to the definition of ϵ, Eq. (1) can be rewritten as an error system

$$\dot{\epsilon}=\mathcal{F}(\epsilon,\tilde{\theta},\tilde{\gamma},e)+Gu_c\tag{38}$$

where $G=[0,0,\ldots,1]^{\mathrm{T}}$ and $\mathcal{F}=[\mathcal{F}_1,\mathcal{F}_2,\ldots,\mathcal{F}_n]^{\mathrm{T}}$ is the aggregate nonlinear system vector field including estimation errors and disturbances. $\mathcal{F}_i = \epsilon_{i+1} + e_{i1} + z_{i1} + \alpha_i + f_i - \dot{\alpha}_{i-1}$, $i = 1, 2, \ldots, n-1$, $\mathcal{F}_n = e_{n1} + \alpha_n + f_n - \dot{\alpha}_{n-1}$, and $\alpha_0 = y_r$.

Following Lemma 1 in Ref. [25], in order to illustrate inverse optimality, two points need to be proved. (1) The controller u_c^* stabilizes the system. (2) The control law can be written in the form $u_c^* = -R^{-1} L_G V^{\mathrm{T}}$ with $R > 0$. In terms of Proposition 2 in Ref. [26], the inverse optimal controller satisfies $u_c = -R^{-1} L_G V^{\mathrm{T}}$. Here, $R^{-1} = k_n + 1 + \hat{\gamma}_n + \dfrac{\Theta_i^{\mathrm{T}} \Theta_i}{2}$.

First, we construct a Lyapunov-HJB structure. A cost function is defined as

$$J(u_c) = \sup\{\lim_{t\to\infty}\{2\beta V(\epsilon) + \int_0^t [l(\epsilon) + u_c^{\mathrm{T}} R u_c]\mathrm{d}\tau\}\} \tag{39}$$

where $l(\epsilon)$ is the running cost defined to match the structure of the HJB inequality. Inspired by inverse optimal theory, select

$$\begin{aligned} l = &-2\beta(L_{\mathcal{F}} V - L_G V R^{-1} (L_G V)^{\mathrm{T}}) + \\ &\beta(\beta - 2) L_G V R^{-1} (L_G V)^{\mathrm{T}} \end{aligned} \tag{40}$$

To establish that the control law u_c^* solves the inverse optimal control problem, it is first to demonstrate that R remains positive definite at all times.

It is not hard to verify from the definition of ξ_i that $\Theta_i^{\mathrm{T}} \Theta_i / 2$ is positive definite. In addition, $\hat{\gamma}_n$ is positive if we choose $\hat{\gamma}_n(0) > 0$. Hence, R is always positive definite.

In light of Theorem 1, the controller in Eq. (32) stabilizes Eq. (1) with $\dot{V} \leqslant -aV + b$. Therefore, for $\forall \|\epsilon\| > \sqrt{2b/a}$, there exists a positive function W satisfying

$$L_{\mathcal{F}} V + L_G V u_c \leqslant -aV + b = -W(\epsilon).$$

According to the LaSalle-Yoshizawa invariant set theorem, one has

$$l \geqslant 2\beta W(\epsilon) + \beta(\beta - 2) L_G V R^{-1} (L_G V)^{\mathrm{T}}.$$

With the fact that $\beta \geqslant 2$, $W(\epsilon)$ is positive definite, l is also positive definite. As a consequence, the cost function in Eq. (39) penalizing on ϵ and u makes sense. Since the controller u_c stabilizes the system, it follows directly that u_c^* also ensures system stability, and thus a formal proof is not required.

Substituting l into Eq. (39), one has

$$\begin{aligned} J = &\sup\{\lim_{t\to\infty}\{2\beta V(\epsilon) + \int_0^t [l + u_c^{\mathrm{T}} R u_c]\mathrm{d}\tau\}\} = \\ &\sup\{\lim_{t\to\infty}\{2\beta V(\epsilon) + \int_0^t [-2\beta(L_{\mathcal{F}} V + L_G V u_c) + \\ &\beta(\beta-2) L_G V R^{-1} (L_G V)^{\mathrm{T}} + u_c^{\mathrm{T}} R u_c]\mathrm{d}\tau\}\} = \\ &\sup\{\lim_{t\to\infty}\{2\beta V(\epsilon) + \int_0^t [-2\beta(L_{\mathcal{F}} V + L_G V u_c) + \\ &\beta^2 L_G V R^{-1} (L_G V)^{\mathrm{T}} - 2\beta L_G V u_c + u_c^{\mathrm{T}} R u_c]\mathrm{d}\tau\}\} = \\ &\sup\{\lim_{t\to\infty}\{2\beta V(\epsilon) - 2\beta \int_0^t \mathrm{d}V + \\ &\int_0^t (u_c - u_c^*)^{\mathrm{T}} R (u_c - u_c^*)\mathrm{d}\tau\}\} = \\ &2\beta V(0) + \int_0^t (u_c - u_c^*)^{\mathrm{T}} R (u_c - u_c^*)\mathrm{d}\tau \end{aligned} \tag{41}$$

It is obvious that the cost function has a minimum value when $u_c = u_c^*$. As a result, u_c^* minimizes the cost function. The value function is $J^*(\epsilon) = 2\beta V(\epsilon)$, i.e., the inverse optimal control problem of Eq. (1) is solvable under the controller in Eq. (32) for all $\|\epsilon\| > \sqrt{2b/a}$. In consequence, u_c^* solves the inverse optimal control problem. This completes the proof. ■

Remark 2 The inverse optimal control problem for nonlinear systems was first formulated in Ref. [3], providing a means to achieve optimal control without the need to directly solve the HJB equation. It is important to emphasize that the design of the inverse optimal controller $u^* = \beta u_c$ must satisfy the following conditions. (1) The derivative of the Lyapunov function $\dot{V}$ remains semi-negative definite under the control input u_c, i.e., $\dot{V} \leqslant 0$. (2) The control law u_c can be expressed in the form $u_c = R^{-1} L_G V^{\mathrm{T}}$, where $R > 0$. (3) The control input is implementable and remains bounded as $L_G V \to 0$, thereby avoiding singularity issues.

IV. Simulation Result

A numerical simulation is conducted in this section to validate the effectiveness of the proposed control strategy.

$$\begin{aligned} &\dot{x}_1 = x_2 + 0.15\sin(0.5t), \\ &\dot{x}_2 = u + x_1^2 + 0.7\sin(t - 3\pi/4) + 1, \\ &y = x_1 \end{aligned} \tag{42}$$

The reference signal is $y_r = \sin(0.5t)$. The controller gains for each step are chosen as $k_1 = 8$ and $k_2 = 15$. Initial values of updating laws are set as $\hat{\theta}_1(0) = [0, 0, \ldots, 0] \in \mathbb{R}^N$ and $\hat{\theta}_2(0) = [0, 0, \ldots, 0] \in \mathbb{R}^N$, $N = 15$ is the dimension of $\hat{\theta}_1$ and $\hat{\theta}_2$. $\hat{\gamma}_1(0) = 0.01$ and $\hat{\gamma}_2(0) = 0.01$. $\Gamma_{11} = 10$, $\Gamma_{12} = 25$, $\Gamma_{21} = 25$, $\Gamma_{22} = 45$, $\sigma_{11} = 1.2$, $\sigma_{12} = 1.0$, $\sigma_{21} = 1.5$, and $\sigma_{22} = 1.5$. The parameters of GPIO are selected as $\lambda_{10} = 80$, $\lambda_{11} = 150$, $\lambda_{20} = 100$, and $\lambda_{21} = 200$.

To highlight the advantages of the proposed GPIO-based inverse optimal controller, comparative simulations are conducted with active disturbance rejection control. The tracking performance and control effort are depicted in Figs. 4 and 5. Figure 4 illustrates the output responses of the closed-loop system with the proposed controller and ADRC. As shown in Fig. 4, the proposed method, which combines the GPIO scheme with a neural network, ensures satisfactory tracking performance, while the ADRC approach demonstrates poor tracking performance. Additionally, Fig. 5 depicts the control input. To further validate the efficacy of the proposed method, Fig. 6 presents the disturbance estimation results, highlighting the adaptive disturbance observer's ability to accurately estimate both matched and mismatched disturbances.

V. Conclusion

A composite optimal control strategy is presented in this paper for a class of uncertain nonlinear systems. To circumvent the complexity of solving nonlinear HJB equations, an inverse optimal control framework is employed. A stabilizing controller is constructed via a modified backstepping technique, from which the corresponding cost function is derived using the Lyapunov-based analysis. Neural networks are utilized to approximate the unknown system dynamics. Furthermore, a GPIO is integrated to estimate disturbances, particularly those that are mismatched. The output of GPIO is embedded into the virtual control design, resulting in a composite controller that enhances system robustness. The proposed method is rigorously analyzed in terms of bounded stability and optimality, with theoretical guarantees provided.

The proposed inverse optimal control framework can be extended to address synchronization challenges in complex dynamical networks, particularly for link synchronization and auxiliary links dynamics. Future research may explore the integration of inverse optimal control with adaptive synchronization strategies developed for uncertain link subsystems (e.g., as discussed in Ref. [27]), aiming to unify optimality and adaptability in network topology control. Moreover, drawing inspiration from approaches where the dynamics of link subsystems assist in the tracking control of node subsystems (e.g., Ref. [28]), the proposed GPIO-based disturbance estimation and composite control design could be extended to enhance robustness in complex dynamical networks with coupled node and link dynamics. These directions offer promising avenues for improving synchronization performance under unmatched disturbances in future networked control systems.

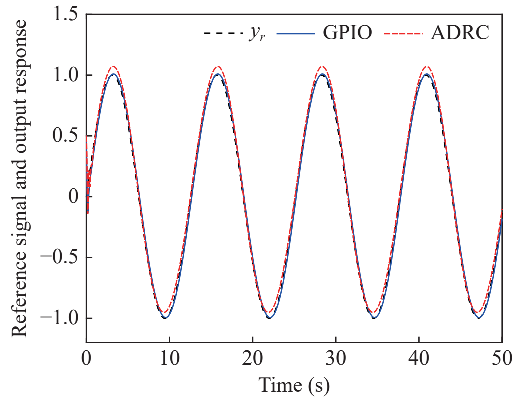

Figure 4 Response curves of system output y and reference signal y_r.

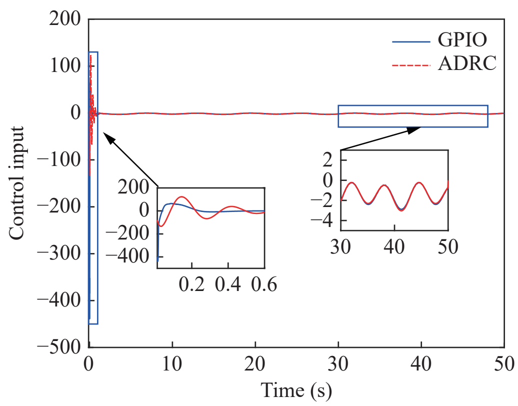

Figure 5 Curve of control input u.

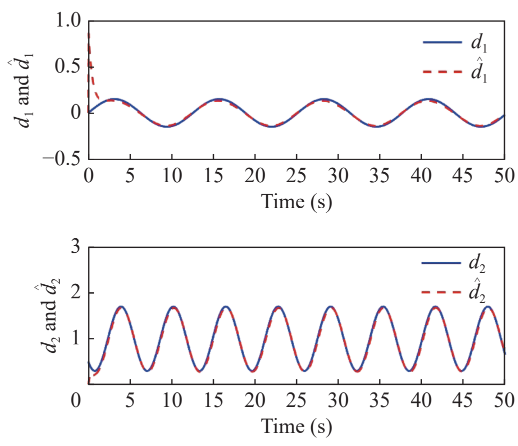

Figure 6 Response curves of real value and estimated value of matched disturbances d_1 and $\hat{d}_1$ and mismatched disturbances d_2 and $\hat{d}_2$.

ACKNOWLEDGMENT

This work was supported by the National Natural Science Foundation of China (No. 62025302).

REFERENCES

[1] N. Ab Azar, A. Shahmansoorian, and M. Davoudi, From inverse optimal control to inverse reinforcement learning: A historical review, *Annu. Rev. Control*, 2020, 50, 119–138.

[2] R. E. Kalman, When is a linear control system optimal, *J. Basic Eng.*, 1964, 86(1), 51–60.

[3] M. Krstic and Z. Li, Inverse optimal design of input-to-state stabilizing nonlinear controllers, *IEEE Trans. Autom. Control*, 1998, 43(3), 336–350.

[4] H. Ma, M. Chen, G. Feng, and Q. Wu, Disturbance-observer-based adaptive fuzzy tracking control for unmanned autonomous helicopter with flight boundary constraints, *IEEE Trans. Fuzzy Syst.*, 2023, 31(1), 184–198.

[5] W. Chen, Disturbance observer based control for nonlinear systems, *IEEE/ASME Trans. Mechatron.*, 2004, 9(4), 706–710.

[6] D. Liu, D. Wang, F. Wang, H. Li, and X. Yang, Neural-network-based online HJB solution for optimal robust guaranteed cost control of continuous-time uncertain nonlinear systems, *IEEE Trans. Cybern.*, 2014, 44(12), 2834–2847.

[7] W. Kang and Q. Gong, Neural network approximations of compositional functions with applications to dynamical systems, arXiv preprint arXiv: 2012.01698, 2020.

[8] W. H. Chen, J. Yang, L. Guo, and S. Li, Disturbance-observer-based control and related methods—An overview, *IEEE Trans. Ind. Electron.*, 2016, 63(2), 1083–1095.

[9] I. Rai, A. Rajendran, A. Lashab, and J. M. Guerrero, Nonlinear adaptive controller design to stabilize constant power loads connected-DC microgrid using disturbance accommodation technique, *Electr. Eng.*, 2024, 106(1), 165–180.

[10] X. Wang and W. Sun, Trajectory tracking of autonomous vehicle: A differential flatness approach with disturbance-observer-based control, *IEEE Trans. Intell. Veh.*, 2023, 8(2), 1368–1379.

[11] Z. Zhou, J. Zhang, Y. Wang, D. Yang, and Z. Liu, Adaptive neural control of superheated steam system in ultra-supercritical units with output constraints based on disturbance observer, *IEEE Trans. Circuits Syst. I: Regul. Pap.*, 2025, 72(6), 2701–2711.

[12] C. Jing, H. Zhang, B. Yan, Y. Hui, and H. Xu, State and disturbance observer based robust disturbance rejection control for friction electro-hydraulic load simulator, *Nonlinear Dyn.*, 2024, 112(19), 17241–17255.

[13] R. X. Zhao, B. Z. Guo, and Q. Q. Hu, Active disturbance rejection control approach to the output tracking of PDEs with general disturbances: A new perspective, *Automatica*, 2024, 164, 111608.

[14] H. Cao, Y. Deng, Y. Zuo, H. Li, J. Wang, X. Liu, and C. H. T. Lee,

Unified interpretation of active disturbance rejection control for electrical drives, *IEEE Trans. Circuits Syst. II: Express Briefs*, 2024, 71(7), 3433–3437.

[15] M. Ali and H. Mirinejad, Robust tracking control of flexible manipulators using hybrid backstepping/nonlinear reduced-order active disturbance rejection control, *ISA Trans.*, 2024, 149, 229–236.

[16] Z. Li, B. Wang, L. Xian, M. Zhang, and Q. Xu, Decentralized active disturbance rejection control for hybrid energy storage system in DC microgrid, *IEEE Trans. Ind. Electron.*, 2024, 71(11), 14232–14243.

[17] J. Sun, Y. Zhang, Y. Chang, T. Shen, and S. Ding, Fixed-time composite learning fuzzy control with disturbance rejection for uncertain engineering systems toward Industry 5.0, *IEEE Trans. Syst. Man Cybern. Syst.*, 2024, 54(7), 4077–4088.

[18] Z. Bao, Y. Zhu, H. Teng, Y. Cui, and L. Guo, Deep-coupled sliding mode disturbance observer-based composite attitude control for flexible communication spacecrafts, *IEEE Trans. Ind. Electron.*, 2025, 72(1), 833–844.

[19] K. Yu, S. Li, W. Zhu, and Z. Wang, Sensorless control scheme for PMSM drive via generalized proportional integral observers and Kalman filter, *IEEE Trans. Power Electron.*, 2025, 40(3), 4020–4033.

[20] J. Sun, J. Yang, W. X. Zheng, and S. Li, GPIO-based robust control of nonlinear uncertain systems under time-varying disturbance with application to DC-DC converter, *IEEE Trans. Circuits Syst. II Express Briefs*, 2016, 63(11), 1074–1078.

[21] Z. Yuan, C. Dai, H. Sun, S. Li, and B. Yin, GPIO based sliding mode control for diesel engine high pressure common rail system, *Int. J. Automot. Technol.*, 2023, 24(1), 147–158.

[22] J. Zhang, X. Liu, Y. Xia, Z. Zuo, and Y. Wang, Disturbance observer-based integral sliding-mode control for systems with mismatched disturbances, *IEEE Trans. Ind. Electron.*, 2016, 63(11), 7040–7048.

[23] M. Krstić, I. Kanellakopoulos, and P. V. Kokotović, *Nonlinear and Adaptive Control Design*, New York, NY, USA: Wiley, 1995.

[24] J. Liu, L. Zhao, S. Li, and R. Liu, Neural network learning-based control for nonlinear systems with time-varying powers, *IEEE Control Syst. Lett.*, 2023, 7, 3579–3584.

[25] K. Lu, Z. Liu, C. L. P. Chen, Y. Wang, and Y. Zhang, Inverse optimal design of direct adaptive fuzzy controllers for uncertain nonlinear systems, *IEEE Trans. Fuzzy Syst.*, 2022, 30(6), 1669–1682.

[26] M. Krstic and P. Tsiotras, Inverse optimal stabilization of a rigid spacecraft, *IEEE Trans. Autom. Control*, 1999, 44(5), 1042–1049.

[27] P. Gao, Y. Wang, J. Zhao, L. Zhang, and Y. Peng, Links synchronization control for the complex dynamical network, *Neurocomputing*, 2023, 515, 59–67.

[28] P. Gao, Y. Wang, Y. Peng, L. Zhang, and S. Li, Tracking control of the nodes for the complex dynamical network with the auxiliary links dynamics, *Inf. Sci.*, 2023, 628, 350–359

Jianan Liu received the BS and MS degrees from Qufu Normal University, China, in 2018 and 2021, respectively. She is currently pursuing the PhD degree at School of Automation, Southeast University, China. Her main research interests include learning-based control and nonlinear control.

Zhongxin Fan received the PhD degree from Southeast University, China, in 2025. Since 2025, he has been an algorithm engineer at SINOMACH Digital Technology Corporation, China. His research interests include anti-disturbance control, optimal control, and learning-based control.

Shihua Li received the BS, MS, and PhD degrees in automatic control from Southeast University, Nanjing, China, in 1995, 1998, and 2001, respectively. Since 2001, he has been with School of Automation, Southeast University, China, where he is currently a professor and the director of the Mechatronic Systems Control Laboratory. He has authored or co-authored over 200 technical papers and two books. He is the chairman of the IEEE IES Nanjing Chapter. He serves as an associate editor or editor of *International Journal of Robust and Nonlinear Control*, *IET Power Electronics*, *International Journal of Control, Automation and Systems*, *International Journal of Electronics*, and *Journal of Power Electronic*, and the guest editor of *IEEE Transactions on Industrial Electrics*, *International Journal of Robust and Nonlinear Control*, and *IET Control Theory and Applications*. He is a fellow of IEEE and a fellow of IET. His research interests include modeling, analysis, and nonlinear control theory with applications to mechatronic systems.

Rongjie Liu received the BS degree in mathematics from Southeast University, Nanjing, China, in 2010, the PhD degree in electrical engineering from The University of Texas at San Antonio, San Antonio, TX, USA, in 2016, and the PhD degree in statistics from Rice University, Houston, TX, USA, in 2020. She is currently an assistant professor at Department of Statistics, University of Georgia, Athens, GA, USA. Her research interests include Bayesian statistics and reinforcement learning.